Chinese Chemical Letters 31 (2020) 2459–2464

Contents lists available at ScienceDirect

Chinese Chemical Letters

journal homepage: www.elsevier.com/locate/cclet

Communication

Enhancement the photovoltaic performance of conjugated polymer based on simple head-to-head alkylthio side chains engineered bithiophene

Zuoji Liu[b,1], Chengjia Bao[a,1], Guangjun Zhang[c], Kai Zhang[a], Gangtie Lei[b,**], Qiang Zhang[a], Qiang Peng[c,**], Yu Liu[a,b,*]

[a] School of Materials Science and Engineering, Jiangsu Engineering Laboratory of Light-Electricity-Heat Energy-Converting Materials and Applications, Jiangsu Collaborative Innovation Center of Photovoltaic Science and Engineering, National Experimental Demonstration Center for Materials Science and Engineering, Changzhou University, Changzhou 213164, China
[b] College of Chemistry, Key Lab of Environment-Friendly Chemistry and Application in the Ministry of Education, Xiangtan University, Xiangtan 411105, China
[c] Key Laboratory of Green Chemistry and Technology of Ministry of Education, College of Chemistry, and State Key Laboratory of Polymer Materials Engineering, Sichuan University, Chengdu 610065, China

ARTICLE INFO

Article history:
Received 16 November 2019
Received in revised form 10 January 2020
Accepted 19 January 2020
Available online 14 February 2020

Keywords:
Bithiophene
Fuorobenzotriazole
Alkoxy side chain
Alkylthio side chain
Polymer solar cells

ABSTRACT

In this article, three novel and simple molecular structure with donor-acceptor (D-A) type copolymers *via* only head-to-head alkoxy (OR) and/or alkylthio (SR) side chains onto the bithiophene (BT) as donor units and fluorinated benzotriazole (FBTA) as acceptor unit, namely, PBTOR-FBTA, PBTOSR-FBTA and PBTSR-FBTA, were successfully designed and synthesized. The impacts of sulfur-oxygen (S···O) or sulfur-sulfur (S···S) noncovalent interactions on their physicochemical properties, molecular stacking, carrier mobility, morphologies of blend films, as well as their photovoltaic performance were deeply and systematically studied. The introduction of SR side-chains suddenly lowered the highest occupied molecular orbital (HOMO) energy levels, blue-shifted absorption, enhanced π-π stacking, as well as improved morphology of the photoactive layer blends in comparison with the reference polymer without SR side-chain. Polymer solar cells (PSCs) were fabricated to estimate their photovoltaic performance of the polymers. Under an optimized blend ratio of PBTSR-FBTA:$PC_{71}BM$ (1:0.8, w/w), the PBTSR-FBTA-based device exhibits a higher power conversion efficiency (PCE) of 6.25%, which is about 3.34 and 1.87 folds than that of the PBTOR-FBTA and PBTOSR-FBTA-based devices, respectively. Our research results demonstrate that the modification of the simple and low-cost SR side chains is an effective strategy to improve the photovoltaic performance of the polymers.

Over the past few years, polymer solar cells (PSCs) have made great progress as a clean renewable energy source, owing to their great advantages for easily fabricating low-cost, light-weight, large-area, and flexible devices through a roll-to-roll process [1–4]. Up to now, the power conversion efficiencies (PCEs) of PSCs are mainly driven by continuous innovation of donor-acceptor materials, interfacial materials and the development of device engineering [5–7]. To the best of our knowledge, the fullerene acceptor ($PC_{71}BM$) itself possesses the advantages of high electron mobility, high electron affinity and charge transport isotropy [8]. Meanwhile, the state-of-the-art of fullerene-PSCs have enabled to achieve PCE up to 11% [9,10]. However, the PCEs still do not meet the commercial application requirements until now. More recently, organic solar cells (OSCs) based on non-fullerene small molecule acceptors (NF-SMAs) have made great progress [11–15]. Particularly, the PCEs based on a single-junction copolymer donor material and ternary tandem polymer-NF-SMAs had been achieved up to 16.5% [13,14] and encouraging, the recordable PCEs of the tandem PSCs have been surpassed 17.3% [15]. Undoubtedly, these successful instances brighten their advantages in the future commercialization of PSCs.

To obtain high efficiency device in PSCs, some crucial challenges still urgent need to solve basic requirement, such as a lower high-lying highest occupied molecular orbital (HOMO) energy level to

* Corresponding authors at: College of Chemistry, Key Lab of Environment-Friendly Chemistry and Application in the Ministry of Education, Xiangtan University, Xiangtan 411105, China.
** Corresponding authors.
E-mail addresses: lgt@xtu.edu.cn (G. Lei), lgt@xtu.edu.cn (Q. Peng), liuyu03b@126.com (Y. Liu).
[1] These two authors contributed equally to this work.

https://doi.org/10.1016/j.cclet.2020.02.021
1001-8417/

improve open-circuit voltages (V_{oc}), a suitable lowest unoccupied molecular orbital (LUMO) energy level to efficiently facilitate charge separation with minimum energy loss, broaden light absorption to increase short-circuit current (J_{sc}), good solubility in organic solvents and high hole mobility to further increase J_{sc} and fill factor (FF), as well as low-cost donor materials [16–19]. Therefore, exploiting simple molecular construction and effective performance copolymer donor materials for PSCs is still particularly urgent [17].

As the electron donor materials of D-A type conjugated copolymers for solar cells, mainly composed of two parts to construct: the π-conjugated skeleton main chain and side chain, in which the π-conjugated backbones mainly determine the PSC related physicochemical properties [15–17,20]. However, in the side-chain engineering of photovoltaic materials, various kinds of simple side chains including alkyl (R), alkoxy (OR), alkylthio (SR) and alkylthienyl groups have a significant role in not only adjusting the solubility of polymers for solution-processed device fabrication, but also in tuning the absorption, energy level, crystallinity and the molecular stacking morphology of the resulting polymers [21–25]. As far as we know, the sulfur (S) atom possesses π-accepting capability, which is mainly due to the $p_{\pi}(C)$-$d_{\pi}(S)$ orbitals overlap of S atom, and its divalent S atom can accept π-electrons from the adjacent C=C orbit to the empty 3 d-orbital [22]. More recently, some reports have demonstrated that the insertion of SR groups on the benzo[1,2-*b*:4,5-*b*′]dithiophene (BDT) can effectively decrease the HOMO level and broaden the light absorption of the copolymers, and thus enhance their photovoltaic performance [23–27]. For example, a highly efficient PSC based on SR side chains functionalized copolymer PBDTTz-SBP presented a PCE of 12.09% [26]. Besides, the devices based on copolymer PNDT-QXS containing SR side chains exhibited a PCE of 5.03% [27]. These is no doubt demonstrate that simple SR substituents can reduce HOMO levels, enhance light absorption and interchain interactions of the corresponding copolymers. Clearly, side-chain engineering is considered a simple and inexpensive strategy to construct D-A type polymers [17–21].

To realize objectives mentioned above, it is feasible to employ for applications of the PSCs by using easy-to-use and cheap materials in the future. So far, some research groups have focused on the low-cost materials that thus jump out of their complicated molecular structures, verbose synthesis steps, and multiple purifications, and realize high efficiency of the PSCs [17,25–33]. For instance, a head-to-head (H···H) linkage containing 3-alkoxy-3'-alkyl-2,2'-bithiophene (TRTOR) as donor unit was reported by Guo group, which is mainly due to the TRTOR unit easily synthesized, low-cost and high coplanarity through intramolecular sulfur-oxygen (S···O) interactions [28,29]. Another example, a H···H linkage involving 3,3'-dialkoxy-2,2'-bithiophene (BTOR) were reported by Meille group, which is primarily attributed to the BTOR unit possessed a better planar structure *via* intramolecular non-covalent S···O interactions [30,26–33]. More recently, a novel easily polythiophene derivatives PBSBT-2 F was designed and synthesized by introducing an simple and cheap SR group into the thiophene, and a PCE of 6.7% was obtained in PSCs based on ITIC acceptor [34]. Obviously, developing simple and efficient polymer donors would be one of the greatest challenges for the application of PSCs.

Here, according to the afore mentioned strategies, three novel conjugated copolymers, namely, PBTOR-FBTA, PBTOSR-FBTA and PBTSR-FBTA, which consist of a simple OR or SR side chains functionlized bithiophene (BT) electron-donating unit and fluorinated benzotriazole (FBTA) as the weak acceptor [16,17,26] (Fig. 1). The alteration of the side chains of the BT unit not only lead to an enhanced coplanarity, but also promote charge mobility, decrease electron density and thus reduce HOMO energy levels [33–37]. The

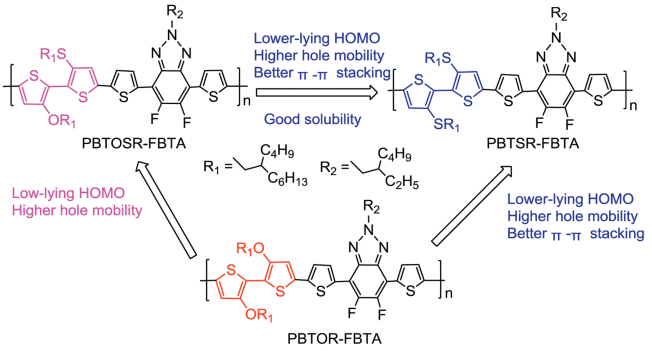

Fig. 1. Chemical structures of the copolymers.

SR-based polymer exhibits a lower-lying HOMO level, higher charge mobility in comparison with its homologous polymers, and resulting in higher V_{oc} and J_{sc} in the PSCs [37–39]. Meanwhile, Under optimized conditions, among the three various FBTA-based copolymers, the PSC based on PBTSR-FBTA/$PC_{71}BM$ (1:0.8, w/w) presents a maximum PCEs of 6.25% with V_{oc} of 0.81 V, J_{sc} of 12.66 mA/cm^2, and FF of 60.94%, which is about 3.34 and 1.87 times higher than that of PBTOR-FBTA and PBTOSR-FBTA based devices, respectively. These obtained values demonstrate that exploiting BT-based copolymers through the reasonable design of side chains is a promising strategy to further tune the optoelectronic properties of the copolymers.

Chemical structures of the copolymers PBTOR-FBTA, PBTOSR-FBTA and PBTSR-FBTA are displayed in Fig. 1, and all copolymers were prepared by Stille-coupling polycondensation according to the synthetic route depicted in Scheme 1. Details of synthesis and structural characterization can be found in Supporting information. At room temperature, both PBTOR-FBTA and PBTSR-FBTA can easily dissolve in common organic solvents, such as CF and chlorobenzene (CB). However, the PBTOSR-FBTA can only dissolve in warm CB solution. The molecular weight and polydispersity index (PDI) of the polymers were evaluated by high-temperature gel permeation chromatography (GPC) using 1,2,4-trichlorobenzene as the eluent and their related data are listed in Table 1. The number-average molecular weights (M_n/kDa) and PDIs of PBTOR-FBTA, PBTOSR-FBTA and PBTSR-FBTA are 12.2/1.51, 68.0/2.37, and 20.5/2.35, respectively. Their thermogravimetric analysis (TGA)

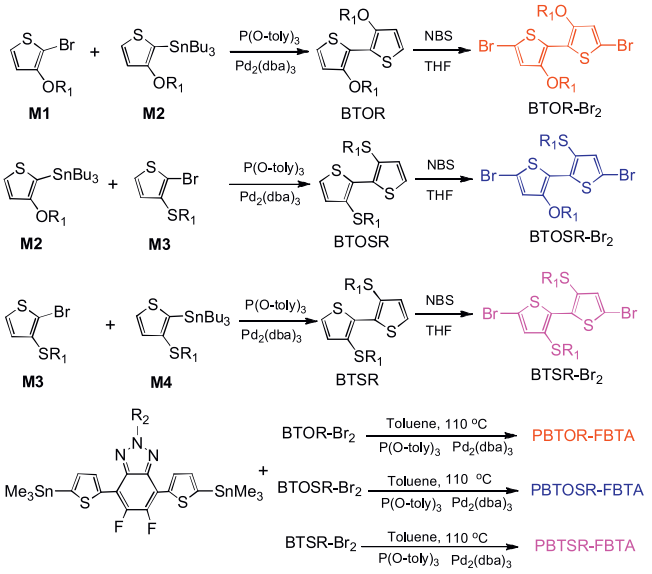

Scheme 1. Synthetic routes to the monomers and copolymers.

Table 1
Molecular weight and thermal properties of the copolymers.

Polymers	M_n (kDa)	M_w (kDa)	PDI	T_d (°C)
PBTOR-FBTA	12.2	18.42	1.51	334
PBTOSR-FBTA	68.0	195.2	2.87	376
PBTSR-FBTA	20.5	48.18	2.35	316

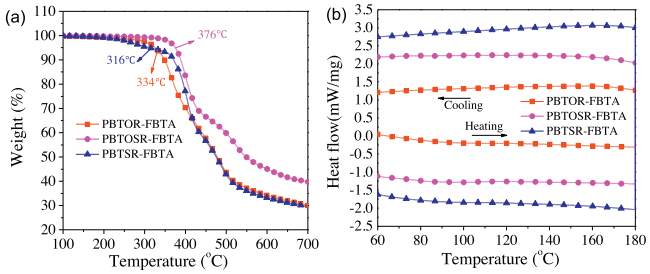

Fig. 2. (a) TGA and (b) DSC curves of copolymers at a scan rate of 10 °C/min under nitrogen atmosphere.

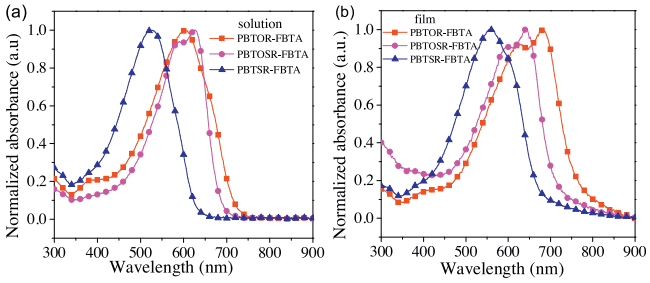

Fig. 3. UV–vis absorption spectra of copolymers in solution (a) and as films (b).

was used to determine thermal stability of the copolymers, as shown in Fig. 2. The decomposition temperature (T_d) of copolymers at 5% weight loss are measured to be 334, 376 and 316 °C for PBTOR-FBTA, PBTOSR-FBTA and PBTSR-FBTA, respectively (Table 1), which indicates that all copolymers have good thermal stability for the employment in PSCs. Moreover, there is neither obvious thermal transition temperature (T_g) nor crystallization temperature (T_c) observed by differential scanning calorimetry (DSC) measurement in the range of 25–180 °C (Fig. 2b), implying that these copolymers display amorphous characteristics.

The absorption spectrum profiles of all copolymers in CF solutions and thin films are shown in Fig. 3, respectively, and the relevant data are listed in Table 2. The PBTSR-FBTA employed S···S side chains engineering based BT group is strikingly blue-shifted but higher band gap compared with the O···O or O···S side chains engineering PBTOR-FBTA and PBTOSR-FBTA, which is assigned to the strong electron-withdrawing ability of SR unit [31]. Meanwhile, the maximum molar absorption coefficient (ε) values of PBTOR-FBTA, PBTOSR-FBTA and PBTSR-FBTA were estimated to be 2.41×10^5 (600 nm), 2.45×10^5 (626 nm), and 2.49×10^5 L mol^{-1} cm^{-1} (524 nm) in CF solutions, respectively, indicating

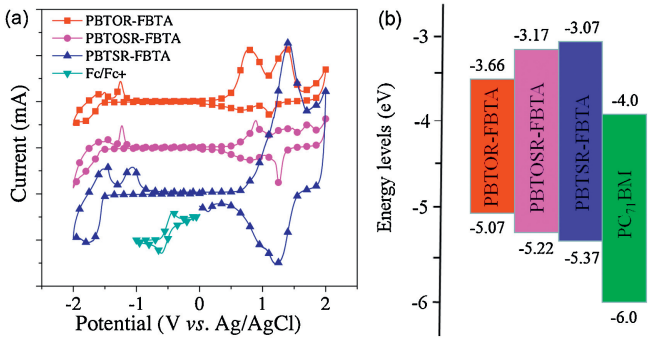

Fig. 4. (a) CV curves of the copolymers at a scan rate of 50 mV/s and (b) schematic energy diagram of the materials used in PSCs.

that the fairly strong absorption ability would be enhanced gradually by introducing S atoms onto the BT group, and mainly due to the strong intermolecular π-π stacking interaction and non-covalent interactions between S···S or S···O in the molecules. Obviously, unexpected influences of copolymers on the absorption performance can also be caused completely through the simple OR and/or SR side-chain engineering, which can make for a much better J_{sc} of PSCs [39]. Meanwhile, significantly red-shifted and lowered band gaps in films compared with in solutions, respectively, mainly owing to the existence of strong π-π aggregation between the molecule frameworks in the all copolymers. As estimated from the absorption onsets of the films, the optical bandgaps (E_g^{opt}) of PBTOR-FBTA, PBTOSR-FBTA and PBTSR-FBTA, are 1.64, 1.74 and 1.87 eV, respectively. What is more, the aggregation of all copolymers was deeper corroborated *via* temperature-dependent absorptions (from 25 °C up to 85 °C) in *o*-dichlorobenzene (*o*-DCB) solution (Fig. S17 in Supporting information). With the increasing of solution temperature from 25 °C to 85 °C, all absorptions of the intramolecular charge transfer (ICT) peaks exhibit blue-shift toward the short wavelength region, and their ratios of $IA_{0\text{-}1}/IA_{0\text{-}0}$ combined with preliminary decreasing, which indicates that these copolymers present different molecular stacking behaviors with a mild changing in the side-chains of the donor units.

The recorded CV curves of copolymers were accomplished by deal with cyclic voltammetry in Fig. 4a and their relevant CV data are outlined in Table 2. The onset oxidation potentials (E_{ox})/onset reduction potentials (E_{red}) of PBTOR-FBTA, PBTOSR-FBTA and PBTSR-FBTA are measured to be 0.60/-0.81, 0.75/-1.30, 0.90/-1.40, respectively [19,20]. The highest occupied molecular orbital (HOMO) level (E_{HOMO}) and the lowest unoccupied molecular orbital (LUMO) level (E_{LUMO}) of these copolymers can be estimated in accordance with the empirical equations: $E_{HOMO} = -(E_{ox} + 4.47)$ eV and $E_{LUMO} = -(E_{red} + 4.47)$ eV [35], and the figured E_{HOMO} and E_{LUMO} values are summarized in Table 2. Clearly, with the replacement of OR side chains with SR side chains, the E_{HOMO} values of the polymers exhibit down-shifted, from -5.07 eV for PBTOR-FBTA, −5.22 eV for PBTOSR-FBTA, to −5.37 eV for PBTSR-FBTA, respectively, which could be assigned to both the spatial

Table 2
Optical and electrochemical properties of the copolymers.

Polymers	λ_{max} (nm)[a]	λ_{max} (nm)[b]	λ_{onset} (nm)[c]	E_g^{opt} (eV)	E_{ox} (V)	E_{red} (V)	E_{HOMO} (eV)	E_{LUMO} (eV)	E_g^{ele} (eV)[c]
PBTOR-FBTA	604	682	757	1.64	0.60	−0.81	−5.07	−3.66	1.41
PBTOSR-FBTA	630	642	712	1.74	0.75	−1.30	−5.22	−3.17	2.05
PBTSR-FBTA	528	557	664	1.87	0.90	−1.40	−5.37	−3.07	2.30

[a] Measured in $CHCl_3$.
[b] Measured in the pure film.
[c] $E_g^{opt} = 1240/\lambda_{onset}$.

hindrance and the electron-deficient effects of SR side chains on the polymer, The lower E_{HOMO} of the polymer donor make for higher V_{oc} of the PSCs [22,36]. Meanwhile, the corresponding E_{LUMO} data of PBTOR-FBTA, PBTOSR-FBTA and PBTSR-FBTA are measured to be −3.66, −3.17, and −3.07 eV respectively. What is more, the electrochemical band gaps (E_g^{ele}) are estimated to be 1.41, 2.05 and 2.30 eV for PBTOR-FBTA, PBTOSR-FBTA and PBTSR-FBTA, respectively, which are well match with the values from the absorption calculations (E_g^{opt}) [34–39]. Fig. 4b presents the energy level diagrams of the copolymers and $PC_{71}BM$ for an evident comparison. It should be noticed that the ΔE_{LUMO} between the three copolymers donor and $PC_{71}BM$ acceptor is 0.34, 0.83 and 0.93 eV PBTOR-FBTA, PBTOSR-FBTA and PBTSR-FBTA, respectively, suggesting that efficient charge separation and transfer could be expected to more occur in the PBTSR-FBTA devices [31–34].

The optimized molecular geometries and electronic distributions of these copolymers were carried out with a chain length of n = 2 at the density functional theory (DFT) B3LYP/6-31G* level with the Gaussian 03 program package [41]. As shown in Fig. 5a, the dihedral (DH) angles between the donor unit and FBTA unit were calculated to be 0.94°, 12.58° and 20.51° for PBTOR-FBTA, PBTOSR-FBTA and PBTSR-FBTA, respectively. Moreover, the DH angles between the central thiophene core and FBTA unit of three copolymers were calculated to be 25.40°, 20.88° and 16.16° for PBTOR-FBTA, PBTOSR-FBTA and PBTSR-FBTA, respectively. The results demonstrated that the PBTSR-FBTA presents a best molecular planarity among all the copolymers, which can facilitate intermolecular π-π stacking and also help the improvement of its FF value. As shown in Fig. 5b, the electron densities of HOMO-1 is mainly concentrated in the core of the bithiophene, and the electron densities of LUMO + 1 is mainly concentrated in the electron-deficient FBTA units. The results demonstrate that the effective charge-transfer process would be possible between the donor and the electron acceptor moieties. The simulated HOMO/LUMO levels were calculated to be -4.708/-2.434 eV, -4.950/-2,506 eV, -5.268/-2.531 eV for PBTOR-FBTA, PBTOSR-FBTA and PBTSR-FBTA, respectively, which the variable trend match well with the tendency of the above CV measurement.

To further understand the effect of various alkyl side chain on the photovoltaic performance of copolymers based PSCs, the hole mobilities (μ_h) of photoactive layers were measured by the space charge limited current (SCLC) method in hole devices with a structure of: ITO/PEDOT:PSS (5000 rpm, 140 °C, 15 min)/copolymer (1200 rpm):$PC_{71}BM$/MoO_3 (10 nm)/Au (100 nm) at the optimized conditions. The SCLC could be estimated using the Mott-Gurney equation: $J = (9/8)\varepsilon_0\varepsilon_r\mu_h(V^2/L^3)$ [41]. The *J-V* curve of the hole-only was shown in Fig. 6 and the measurement results were listed in Table 3. The PBTSR-FBTA/$PC_{71}BM$ blend film exhibits highest μ_h of 3.62×10^{-4} $cm^2 V^{-1} s^{-1}$ than the PBTOR-FBTA/$PC_{71}BM$ and PBTOSR-FBTA/$PC_{71}BM$ blend films of 3.96×10^{-5} and 9.77×10^{-5} $cm^2 V^{-1} s^{-1}$, respectively. Obviously, the highest μ_h of the PBTSR-FBTA copolymer match with the strong interchain interaction of the polymer and the highest J_{sc} value of the corresponding PSCs.

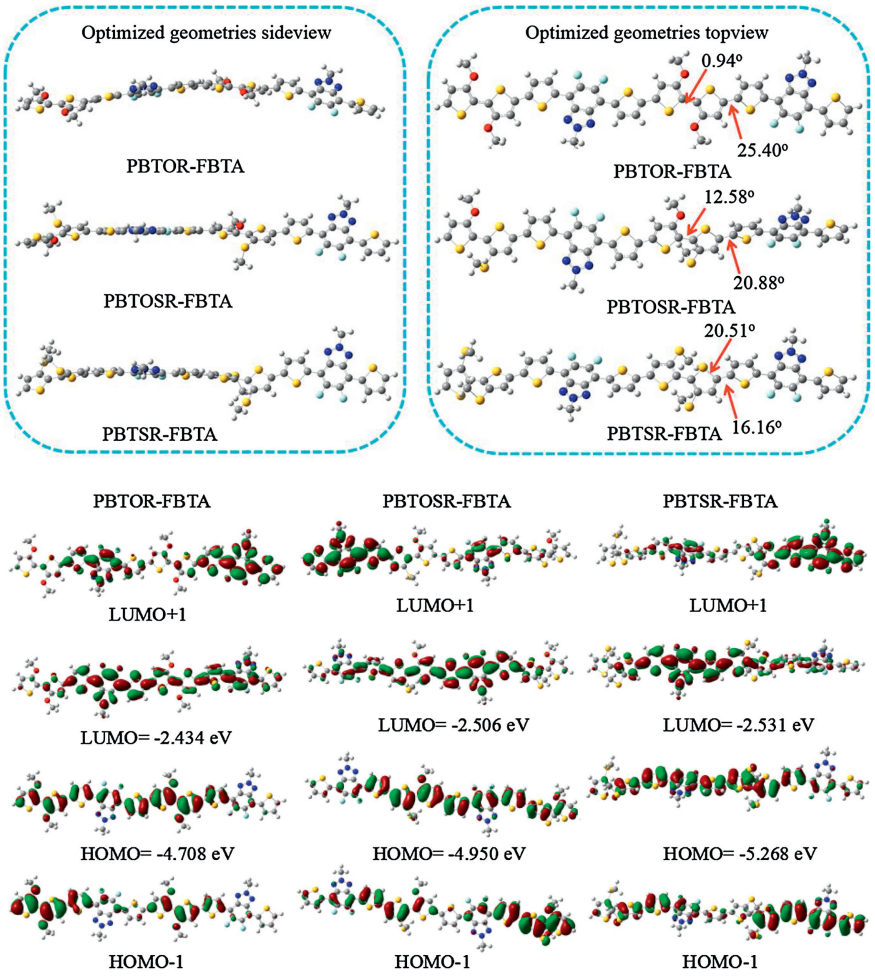

Fig. 5. (a) Optimized molecular geometries and (b) molecular frontier orbitals of LUMO + 1, LUMO, HOMO, and HOMO-1 for copolymers obtained by Gaussian 09 at the B3LYP/6-31 G(d) level.

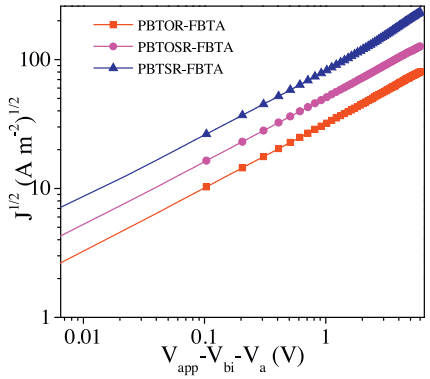

Fig. 6. *J-V* curves of the optimized hole-only copolymers/$PC_{71}BM$ devices.

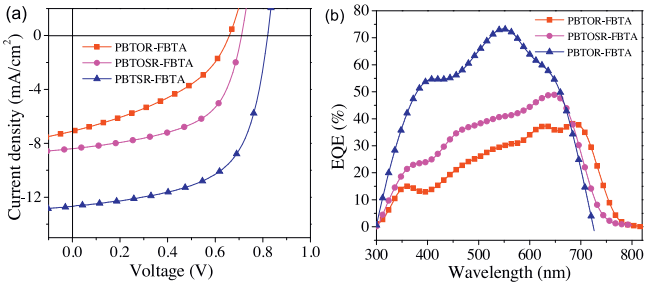

Fig. 7. (a) *J-V* curves and (b) EQE spectra of the copolymers/$PC_{71}BM$ cells at the optimized copolymers/$PC_{71}BM$ devices under AM.1.5 G illumination (100 mW/cm^2).

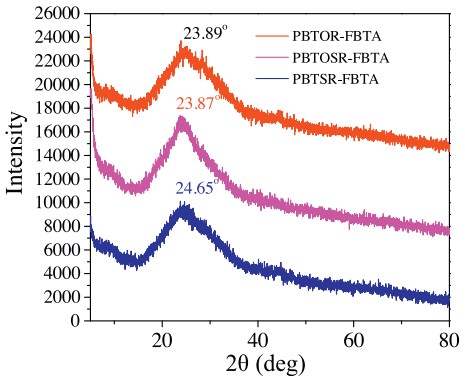

Fig. 8. XRD patterns of the pure copolymer films on silicon wafers.

To research the effect of OR or SR side chains on the photovoltaic performance, under simulated air mass 1.5 global (AM 1.5 G, 100 mW/cm^2) irradiation, PSCs are fabricated appointing conventional architectures, specifically indium tin oxide (ITO)/ZnO (5000 rpm, 180 °C, 30 min)/copolymer:$PC_{71}BM$ (1200 rpm)/MoO_3/Ag. The active layer of copolymer/$PC_{71}BM$ was obtained from chlorobenzene (CB) solution at a concentration of 15 mg/mL. Photovoltaic performances of PSCs were strongly influenced by some processing parameters, such as the solvent selection, the D/A (copolymer/$PC_{71}BM$, w/w) blend ratio, the annealing temperature, the spin-coating rates, the usage of processing additives. The *J-V* characteristics of the copolymers:$PC_{71}BM$-based those optimized devices and their corresponding photovoltaic data are exhibited in Figs. S11-S16 (Supporting information) and in Tables S1-S6 (Supporting information), respectively. As a result, the optimized devices for PBTOR-FBTA, PBTOSR-FBTA and PBTSR-FBTA solar cells D/A blend ratio are 1:0.8, 1,8-octanedithiol (DIO) additive concentration of 0.2%, spin-coating rate of 1200 rpm, respectively. The current density-voltage (*J-V*) characteristics and EQE curves of the optimized devices are presented in Fig. 7, and their corresponding photovoltaic data are also listed in Table 3, respectively. As shown in Fig. 7a, the OR functionalized BTOR-FBTA devices presents a lower PCE of 1.87% with a V_{oc} of 0.65 V, a J_{sc} of 7.10 mA/cm^2, and an FF of 40.49%. When using SR engineered PBTOSR-FBTA instead of PBTOR-FBTA, the PCE, V_{oc}, J_{sc} and FF values were found to be enhanced simultaneously (PCE: 3.35%; V_{oc}: 0.71 V; J_{sc}: 8.41 mA/cm^2; FF: 56.10%). Particularly, the double SR substitutional PBTSR-FBTA-based devices exhibited a largest V_{oc} of 0.81 V, J_{sc} of 12.66 mA/cm^2, and FF of 60.94%, and triggering a much highest PCE of 6.25%. Obviously, from all the devices, the significant enhancements of V_{oc}, J_{sc} and FF values of PBTSR-FBTA based device should be ascribed to the gradually reduced HOMO levels, improved charge transport, as well as a better planarity with a good π-π stacking.

Their EQE profiles of the corresponding PSCs, were showed in Fig. 7b and the related data were listed in Table 3, similar shape ranging from 300 nm to 800 nm for PBTOR-FBTA and PBTOSR-FBTA, and 300–730 nm for PBTSR-FBTA blending films, respectively. The PBTSR-FBTA-based PSCs exhibits a EQE of 73.2% at 552 nm, which is higher than the value of 38% at 685 nm for PBTOR-FBTA, 49.4% at 648 nm for the PBTOSR-FBTA-based devices, respectively. Clearly, suggesting that PBTSR-FBTA confers the maximum contribution to the J_{sc} value among the three copolymer donors. The integrated J_{sc} for PBTOR-FBTA, PBTOSR-FBTA and PBTSR-FBTA solar cells are to be 6.93, 8.41 and 12.15 mA/cm^2, respectively, which all match well with those values achieved from the *J-V* curves within 5% error.

To evaluate the dissociation of excitons, steady-state photoluminescence (PL) spectroscopy was used to study the charge dissociation of photocurrent conversion. The PL spectra of the polymers PBTOR-FBTA, PBTOSR-FBTA and PBTSR-FBTA, acceptor $PC_{71}BM$ film and their blend films were measured at different excitation wavelengths. The excitation wavelength of the three blend films of PBTOR-FBTA, PBTOSR-FBTA and PBTSR-FBTA is 600 nm, and that of the acceptor $PC_{71}BM$ is 500 nm. As shown in Figs. S18a–c (Supporting information), the emission of PBTSR-FBTA was completely quenched by $PC_{71}BM$, implying that the electrons can transfer efficiently to $PC_{71}BM$. Nevertheless, the emission of PBTOR-FBTA and PBTOSR-FBTA are not completely quenched by $PC_{71}BM$, and leading to the lowest J_{sc}. The results show that the excitons of the PBTSR-FBTA blend film can be effectively dissociated, thereby increasing J_{sc} and FF.

Their crystalline natures and molecular orientations of these copolymers in the solid states were tested with X-ray diffraction (XRD). As shown in Fig. 8, PBTOR-FBTA, PBTOSR-FBTA and PBTSR-FBTA display a distinct and broad (010) peaks at 2θ = 23.89°, 23.87° and 24.65°, which were attributed to the (010) diffraction from a

Table 3
Photovoltaic and hole mobility data of the optimized devices based on copolymers.[a].

Active layer	V_{oc} (V)	J_{sc} (mA/cm^2)	FF (%)	PCE (%)	μ_h (cm^2 V^{-1} s^{-1})
PBTOR-FBTA:$PC_{71}BM$	0.65	7.10	40.49	1.87(1.58)	3.96×10^{-5}
PBTOSR-FBTA:$PC_{71}BM$	0.71	8.41	56.10	3.35(3.05)	9.77×10^{-5}
PBTSR-FBTA:$PC_{71}BM$	0.81	12.66	60.94	6.25(6.01)	3.62×10^{-4}

[a] Blending with $PC_{71}BM$, annealing at 140 °C, spin-coating rate 1200 rpm, 15 mg/mL in solvent CB, 0.2% DIO used as additive.

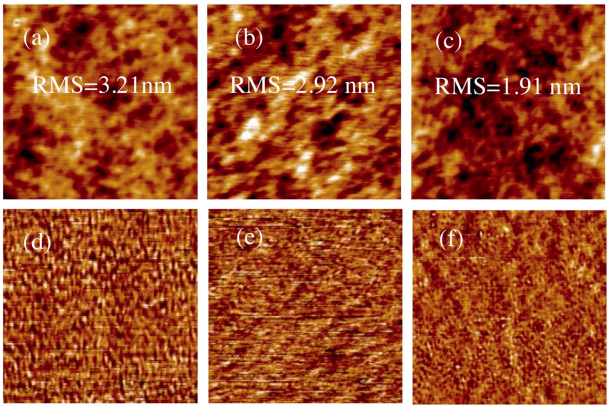

Fig. 9. AFM height images (a, b, c) and phase images (d, e, f,) of the copolymers-based active blends.

lamellar packing. Moreover, the corresponding π-π stacking distances (d_π) between the coplanar skeletons of copolymers are also obtained to be 3.73 Å, 3.72 Å and 3.60 Å for PBTOR-FBTA, PBTOSR-FBTA and PBTSR-FBTA, respectively. Indeed, a much smaller d_π value was observed for the PBTSR-FBTA than that for the PBTOR-FBTA and PBTOSR-FBTA, indicating that the inserted double SR group effectively enhanced the π-π stacking performance of the corresponding PBTSR-FBTA, and make for the improvement of μ_h in the related devices. These results agree well with the DFT theoretical calculations and the μ_h values of the corresponding copolymers mentioned above, which should be advantageous to ameliorate its J_{sc} and FF values in PSCs [36].

Further endeavor was required to disclose the surface and bulk morphology of the active blend films, so the atomic force microscopy (AFM) in a surface area of $5 \times 5\,\mu m^2$ was used for determining. As shown in Fig. 9, the root mean square (RMS) roughness from the height images were determined as 3.21, 2.92 and 1.91 nm for the PBTOR-FBTA, PBTOSR-FBTA and PBTSR-FBTA-blended films, respectively. Among them, the PBTSR-FBTA film reveals a much smoother roughness than that of the other copolymers, which would strengthen the exciton dissociation and charge transport efficiency, and thus resulting in the enhanced J_{sc} and FF for the higher PCE [39–41]. Unquestionably, the simple SR functionlized bithiophene donor unit should be entirely possible applied as promising donor unit *via* copolymerizing group with other acceptors for highly efficient PSCs.

In conclusion, we have exhibited the synthesis and photovoltaic properties of a simple bithiophene derivatives, copolymers PBTOR-FBTA, PBTOSR-FBTA and PBTSR-FBTA, based on OR and/or SR side chains substituted bithiophene donor unit and FBTA as acceptor unit, respectively, for researches on the relationship of the molecular structure and photovoltaic properties of the copolymer photovoltaic materials. The substitution of a SR side chains on the bithiophene unit in the copolymers was found to making for higher absorption, lower HOMO level, better molecular stacking, and higher mobility in comparison with the copolymers analogues with OR side chains on the bithiophene unit, which is conducive to improving the V_{oc}, J_{sc} and FF in PSCs simultaneously. Under optimization, the PSC based on PBTSR-FBTA/$PC_{71}BM$ (1:0.8, w/w) presents a maximum PCE of 6.25% with a V_{oc} of 0.81 V, a J_{sc} of 12.66 mA/cm^2 and an FF of 60.94%, which is about 3.34 and 1.87 times higher than that of PBTOR-FBTA and PBTOSR-FBTA based devices, respectively. Our results demonstrate that the simple BTSR unit should be a promising donor unit for future applications of PSCs.

Declaration of competing interest

There are no conflicts to declare.

Acknowledgments

This work was financially supported by grants from the National Natural Science Foundation of China (Nos. 51573154, 51673031), The Natural Science Foundation of Jiangsu Higher Institutions of China (No. 18KJA480001), the Youth Science and Technology Foundation of Sichuan Province (No. 2013JQ0032), the key Laboratory of Environment-Friendly Chemistry and Applications of Ministry of Education (No. 2018HJYH01), the Natural Science Foundation of Jiangsu Province (No. BK20141151).

Appendix A. Supplementary data

Supplementary material related to this article can be found, in the online version, at doi:https://doi.org/10.1016/j.cclet.2020.02.021.

References

[1] G. Li, R. Zhu, Y. Yang, Nat. Photon. 6 (2012) 153–161.
[2] K.A. Mazzio, C.K. Luscombe, Chem. Soc. Rev. 44 (2015) 78–90.
[3] F. Liu, Z. Du, X. Yuan, et al., Polymer 168 (2019) 1–7.
[4] X. Xu, G. Zhang, Y. Li, et al., Chin. Chem. Lett. 30 (2019) 809–825.
[5] Z. Xiao, X. Jia, D. Li, et al., Sci. Bull. 62 (2017) 1494–1496.
[6] L. Lu, T. Zheng, Q. Wu, et al., Chem. Rev. 115 (2015) 12666–12731.
[7] N. Wang, W. Yang, S. Li, et al., Chin. Chem. Lett. 30 (2019) 1277–1281.
[8] C. Lee, S. Lee, G.U. Kim, et al., Chem. Rev. 119 (2019) 8028–8086.
[9] J. Zhao, Y. Li, G. Yang, et al., Nat. Energy 1 (2016) 15027.
[10] T. Kumari, S.M. Lee, S.H. Kang, et al., Energy Environ. Sci. 10 (2017) 258–265.
[11] M. Luo, C. Zhu, J. Yuan, et al., Chin. Chem. Lett. 30 (2019) 2343–2346.
[12] Y. Cui, H. Yao, L. Hong, et al., Adv. Mater. 31 (2019) 1808356.
[13] Y. Cui, H. Yao, J. Zhang, et al., Nat. Commun. 10 (2019) 2515.
[14] R. Yu, H. Yao, Y. Cui, et al., Adv. Mater. 31 (2019) 1902302.
[15] L. Meng, Y. Zhang, X. Wan, et al., Science 361 (2018) 1094–1098.
[16] Y. Lin, F. Zhao, Y. Wu, et al., Adv. Mater. 29 (2017) 1604155.
[17] H. Bin, Y. Yang, Z. Peng, et al., Adv. Energy Mater. 8 (2017) 1702324.
[18] Y. Liu, J. Zhao, Z. Li, et al., Nat. Commun. 5 (2014) 6293.
[19] Q. Fan, H. Jiang, Y. Liu, et al., J. Mater. Chem. C 4 (2016) 2606.
[20] J. Yu, J. Cao, H. Tan, et al., Dye. Pigment. 141 (2017) 21–28.
[21] P. Zhu, B. Fan, X. Du, et al., ACS Appl. Mater. Interfaces 10 (2018) 22495–22503.
[22] J. Wan, X. Xu, G. Zhang, et al., Energy Environ. Sci. 10 (2017) 1739–1745.
[23] C. Cui, Z. He, Y. Wu, et al., Energy Environ. Sci. 9 (2016) 885–891.
[24] G. Huang, J. Zhang, N. Uranbileg, et al., Adv. Energy Mater. 8 (2017) 1702489.
[25] G. Zhang, X. Xu, Z. Bi, et al., Adv. Funct. Mater. 28 (2018) 1706404.
[26] W. Chen, G. Huang, X. Li, et al., ACS Appl. Mater. Interfaces 10 (2018) 42747–42755.
[27] Y. Lin, X. Chen, C. Jiang, et al., Org. Electron. 61 (2018) 197–206.
[28] X. Guo, Q. Liao, E.F. Manley, et al., Chem. Mater. 28 (2016) 2449–2460.
[29] X. Guo, J. Quinn, Z. Chen, et al., J. Am. Chem. Soc. 135 (2013) 1986–1996.
[30] H. Huang, L. Yang, A. Facchetti, et al., Chem. Rev. 117 (2017) 10291–10318.
[31] T.L. Nguyen, H. Choi, S.J. Ko, et al., Energy Environ. Sci. 7 (2014) 3040–3051.
[32] H. Xin, X. Guo, G. Ren, et al., Adv. Energy Mater. 2 (2012) 575–582.
[33] H. Xin, X. Guo, F.S. Kim, et al., J. Mater. Chem. 19 (2009) 5303–5310.
[34] Q. Xu, C. Chang, W. Li, et al., Acta Phys. Chim. Sin. 35 (2019) 268–274.
[35] R.L. Uy, L. Yan, W. Li, et al., Macromolecules 47 (2014) 2289–2295.
[36] S. Tan, X. Wu, Y. Zheng, et al., Chin. Chem. Lett. 30 (2019) 1951–1954.
[37] I. Meager, R.S. Ashraf, S. Mollinger, et al., J. Am. Chem. Soc. 135 (2013) 11537–11540.
[38] T. Yu, X. Xu, G. Zhang, et al., Adv. Funct. Mater. 27 (2017) 1701491.
[39] Y. Zou, Y. Dong, C. Sun, et al., Chem. Mater. 31 (2019) 4222–4227.
[40] S. Jin Ko, Q.V. Hoang, C.E. Song, et al., Energy Environ. Sci. 10 (2017) 1443–1455.
[41] K. Li, Z. Li, K. Feng, et al., J. Am. Chem. Soc. 135 (2013) 13549–13557.